International Journal of Engineering Science Invention (IJESI)
ISSN (Online): 2319 – 6734, ISSN (Print): 2319 – 6726
www.ijesi.org ||Volume 8 Issue 03 Series. II || March 2019 || PP 01-10

Estimation of Tropospheric Propagation Delay for Long Base Line in Gps Positioing

Jinseok Hong[1], Miae Ha[2]
[1]*Department of Engineering, Engineering Technology, and Surveying, East Tennessee State University, Tennessee, USA*
[2]*Water Management and Hydrological Science, Texas A&M University, College Station, Texas, USA*
Corresponding Author: Jinseok Hong

Abstract: *The Global Positioning System (GPS) has been used to determine highly accurate static and aircraft positions for gravimetric, photogrammetric, LiDAR and many other applications. This level of precision can be achieved using two or more GPS receivers and carrier phase differencing techniques. However, residual tropospheric propagation delay can still contribute a bias in height of several centimeters even if simultaneously recorded meteorological data are used. This shortcoming is primarily due to the complexity of the water vapor profile in the tropospheric delay models. Tropospheric delay is a function of the tropospheric refractive index, which is dependent on the local temperature, barometric pressure and relative humidity. This experiment was conducted to analysis the effects of tropospheric delay over long base lines using real-time barometric pressure data. One key to making this evaluation was to assess the height difference between the data processed with barometric pressure and processed without barometric pressure. Although the statistical results of the position difference between the local base station and the station at the University of Florida, with and without barometer data were less then desired or expected, it has been demonstrated that under proper conditions it might improve accuracy of aircraft positions over long base line.*

Keywords *–GPS, tropospheric delay, long base line, Lidar*

Date of Submission: 20-02-2019 Date of acceptance: 05-03-2019

I. INTRODUCTION

The Global Positioning System (GPS) is satellite-based radio-positioning and time-transfer system designed, financed, deployed, and operated by the U.S. Department of Defence (DOD) for military and civilian applications. With the increasing use of the GPS applications, all the potential error sources of the system need to be understood. GPS satellite signals travel thought various layers of the atmosphere during transmission from the satellites to the receivers on or near the surface of the Earth. One of the most significant problems is the effect of the neutral-atmosphere on the GPS signals traveling between satellites and receivers. The effect is to both changing the velocity of the signal and refracting (bending) its ray path. The effects on geodetic-type static positioning are generally well known and special considerations may exist for airborne positioning [1]. The more general effect on a GPS receiver at arbitrary height above the earth's surface must be considered for airborne positioning.

The particular problems in airborne GPS positioning are: 1) the change of the tropospheric propagation delay with a change in height, and 2) the usual lack of direct meteorological data to help quantify the state of the atmosphere [2]. The troposphere is the lowest part of the Earth atmosphere, extending up to about 50 km above the surface. The troposphere is part of the electrically neutral (neither ionized nor dispersive) layer for propagation of electromagnetic waves with frequencies below 30 GHz, as for instance GPS signals [3, 4]. Therefore, both L1 and L2 are equally refracted. In addition to the dispersive ionosphericdelay the tropospheric delay is one of the most difficult-to-model errors affecting space geodetic techniques. The zenith tropospheric propagation delay is usually split into two components, designated as hydrostatic (or dry) and wet. The hydrostatic part of the delay is approximately 90 % of the total tropospheric propagation delay and wet part of the delay is approximately 10 % of the total delay [5]. Each one consisting of the product of the delay at the zenith and a mapping function that projects the zenith delay to the desired line-of-sight. In general, these mapping functions are parameterized by specific meteorological or other site-dependent parameters that can be readily determined [6].

A number of tropospheric propagation delay models, zenith delay models and mapping functions have been developed for use in the analysis of modern space geodesy techniques, such as the GPS, Very Long Baseline Interferometry (VLBI), Doppler Orbitography and Radiopositioning Integrated by Satellite (DORIS), Satellite altimetry, and Satellite Laser Ranging (SLR) [7, 8, 9, 10]. An unmodeled tropospheric propagation

delay affects mainly the height component of position and constitutes therefore a matter of concern in space-geodesy applications, such as sea-level monitoring, postglacial rebound measurement, earthquake-hazard mitigation, and tectonic-plate-margin deformation studies [6, 11]. The mitigation of the tropospheric effects will increase the prospect of more accurate and precise airborne GPS positioning. In post-processing dual frequency GPS carrier phase data, the residual tropospheric delay can easily be the largest remaining error source [2]. So even though the hydrostatic (dry) component of the tropospheric zenith delay can be modeled to millimeter accuracy, this requires an accurate atmospheric pressure measurement. If any tropospheric model is used due to lack of real pressure values, it will introduce a bias into the delay determination. The tropospheric propagation delay of satellite signals is a function of local temperature, barometric pressure and atmospheric water vapor, and modeling the troposphere is one way to reduce the bias in GPS data processing up to 95 percent effective [12]. For these reasons, it might be necessary to take account for measurements of real time barometric pressure data for high-precision applications such as light detection and ranging (LiDAR).The tropospheric propagation delay will be practically eliminated by double differencing for short baselines but for long baselines the residual tropospheric propagation delay will have a substantial size, and it has to be considered in the data processing [3].

The objectives of this project are to evaluate the potential impact on an aircraft's position caused by tropospheric propagation delay from barometric pressure. One key to making this evaluation was to assess the height difference between the data processed with barometric pressure and processed without barometric pressure. These objectives include determination the bounds of the tropospheric delay contribution to the accuracy of aircraft positions over long base line.

II. MATERIALS AND METHODS

2.1. Project location and data collection

The site chosen for this project is in Jacksonville, Florida, which is about 110 kilometers (69 miles) northeast of the reference station along Florida's east coast. (Fig. 2.1).

Fig. 2.1: Location of the project area in Jacksonville, FL

Dual-frequency (L1 and L2) GPS data were collected at a collection rate of one hertz and 15º cut off angle on the airplane and the reference station, Natasha (NATA). Within the project site one receiver was positioned at the Apalachicola Municipal Airport on station APALPORT (PID# AS0884) and the other receiver (as a backup) was on a new point established by GPS observations on the previous day. This new point named PT01 is occupied in an open grassy field near the intersection of SR65 and Tower Road, across the road from the Tate's Hell ranger station and fire lookout tower. The GPS observation started around 08:00 AM to 11: 50 AM EST and the weather was clear, cool (4 to 12°C), and breezy, and the collection proceeded normally.

2.2. Reference station

One GPS receiver (Ashtech Z-12) is running 24 hours a day and the choke ring antenna is attached to the receiver with a 25-meter RG-8/50 ohm coaxial cable and is mounted to a fixed pedestal on the roof of Reed laboratory as a reference station (NATA) at the University of Florida (UF). Fig. 2.2 shows the setting when data were collected at the reference station and Table 2.1 shows coordinates of NATA as the reference station.

Fig. 2.2: The reference station settings

Table 2.1: Coordinates of the NATA

Earth-Centered Cartesian Coordinates (Meter)			Geodetic Coordinates		
X	Y	Z	Latitude	Longitude	Ellipsoid Height
738692.446	5498291.522	3136525.402	29°38’52.417”N	82°20’53.382”W	26.479 m

2.3. Rover

The UF Cessna 337 Skymaster in line twin engine aircraft is equipped with a Starlink real time GPS navigation unit, and an L1/L2 microstrip antenna for geodetic quality GPS phase difference observations is used as a rover for this project.The barometer was resting on top of laser sensor head that is next to the pilot seat to collect barometric pressure data for outside of the aircraft. Fig. 2.3 shows the rover with the barometer at the hanger.

Fig. 2.3: Rover with the barometer

2.4. Barometer

Since the availability of reliable barometric pressure is one of keys for this research, one high accuracy digital barometer was set up on the aircraft and the other one was set up next to the antenna at the reference station. The PTB220 series digital barometer from Vaisala, Inc. used for this project is a fully compensated digital barometer designed to cover a wide range of environmental pressure and temperature.

HyperTerminal, a communication program, was used to control the barometer settings. The program, Get Pressure and Time (GPT), reads time synchronized with Greenwich Mean Time (GMT) from the computers and barometric pressure data from the barometers so they can display both time and pressures in a text file (data.tmp). GPT was modified to collect and record specific format as KARS requires in the order of date, time and barometric pressure (mbar) data. Both airborne and ground barometric pressure data were collected at 10-second intervals.

2.5 Kinematic and Rapid-Static (KARS)

The key to process and get a precise trajectory of aircraft in this project is Kinematic And Rapid-Static (KARS) GPS processing software programmed by Dr. Gerald L. Mader, at the National Geodetic Survey (NGS) to allow for the estimation of the tropospheric delay for this project. KARS utilizes an optimized integer search technique that examines the number of possible integer combinations within a search volume and an ion window. KARS also needs dual-frequency (L1 and L2) GPS observations to process. To minimize satellite position error as much as possible, International GPS service for Geodynamics (IGS) precise orbits and double differencing method is used for kinematic trajectory in KARS.

The tropospheric delay model KARS uses is the old Marini model that has identical mapping function to newer tropospheric models above 15 degree elevation. There are several input files for KARS and Table 2.2 shows some functions of input files.

Table 2.2: Functions of KARS input files

Name of input files	Functions
Kinpos.inp	File specifying start/stop times of processing, location of data files, run options and plot operations
Param	File containing the numerical values of various parameters
Phifix	File containing the values of the integer bias, if known, at a particular time to start the phase solution without an OTF ambiguity search. This file is optional.
Kars.edt	File containing edits instructions for the kinpos program. This file is optional and is usually used to delete bad data.
Ant_info.003	File containing antenna offsets and phase center variations with elevation for a catalog of standard antennas.
****###*. ##o	RINEX observation files for the rover and reference data
****###*. ##n	RINEX navigation file
****###*. Sp3	Standard sp3 format file for satellite ephemeredes.

In order to process GPS data with KARS, Receiver Independent Exchange (RINEX) format observation files for a rover and base station, a precise ephemeris, RINEX navigation file, barometric data file for rover and base station, and an antenna offset file are needed.Range solution must be run between the base station and rover. Range solution will not have the sub-decimeter accuracy needed for precise positioning, but will have meter level accuracy necessary for further data analysis [13]. Range solution creates “rsolxyz” file. This file contains the vectors that can be applied to the base station’s geocentric coordinates to determine the x, y and z coordinates of the rover [13]. Fig. 2.4 is an example result of range solution.

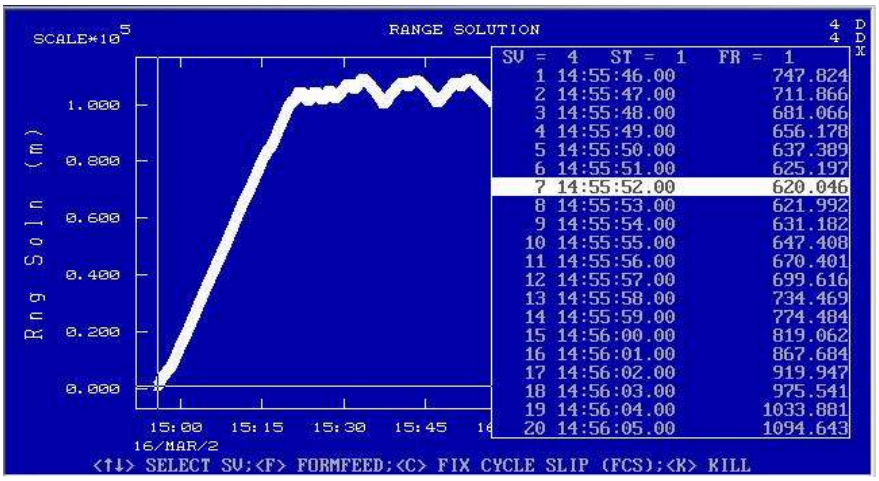

Fig. 2.4: Range solution window

Fixing integer combinations from the "integers" file in the "phifix"file, editing with "kars.edt", and setting the ionospheric window in the "param" file need to be set depends on result of range solution. KARS always holds the satellite with the highest elevation as reference satellite for the double difference solution [13]. Using the nearest points from base station for initialization phase solution could be processed under an assumption that if the rover and base station are within close proximity, such as less than ten kilometers, the change in the ionosphere between the base station and the rover will be small. Once initialization is done, and as long as there are no cycle slips or loss of lock, the aircraft's position can be precisely calculated one hundred or more kilometers from the base station. The equation for Marini tropospheric delay model is as following.

$$TDC = \frac{1}{FC} \times \frac{A + B}{Sin E + \frac{B}{\frac{A+B}{Sin E + 0.015}}}$$

Where

FC = 1-0.0026 cos2ϕ -0.00031 H

$$A = 0.002277 \times \left(P_0 + \left(\frac{1255}{T} + 0.05 \right) \times E_0 \right)$$

$$B = 0.002644 \times e^{-0.14372 \times H}$$

Where

TDC = range correction due to the tropospheric propagation delay

ϕ = the geodetic latitude of the site

H = the height above the geoid (Km)

E = the geometric elevation of the observation in radian

P_o = atmospheric pressure (milibars)

T = temperature (Kelvin)

E_0= water vapor pressure (milibars)

Where

$$E_0 = (R_h/100) \times E_s$$

$$E_s = 6.11 \times 10^{7.5 \times \frac{T - 273.16}{T - 35.86}}$$

Water vapor pressure can be calculated from saturation vapor pressure, $E_s$and R_h is relative humidity measurement (%).

III. RESULTS AND DISCUSSION

Information such as satellite elevation, phase and range residuals, available satellites and L1 ionosphere correction can be viewed in its native ASCII format as well as graphically in the SPLOT program, which is included with KARS.A set of fixed carrier phase integer ambiguities for all available satellites during the flight on both frequencies was derived. This was done by processing the flight data at elevation cut-off angle 15

degree while resolving the ambiguities "on-the fly". These ambiguities could be confirmed by examining the residuals of the position solution to see if they diverge over time.

Like all electromagnetic waves, the GPS signals are delayed in the troposphere and the ionosphere and the ray paths are bent because of variations in the index of refraction. In the ionosphere, this variation is due to the varying electron content and in the neutral atmosphere, the index of refraction of electromagnetic waves is a function of temperature, pressure, and water content (humidity).

Table 3.1 shows a summary of the statistics including distance from the base station, number of observations, root mean square error (RMSE) for rover's positions and position dilution of position (PDOP).

Table 3.1: Jacksonville project data set

Maximum Distance from base station (Km)	Number of observations (second)	RMSE (Meter)		PDOP		
		Average	Standard deviation	Min	Average	Max
109	7000	0.015	0.008	1.7	2.5	4.3

Total number of observations for Jacksonville project was from 14:55:46 to 16:52:25 GMT (7000 seconds) with average 0.015 meter RMSE. Average PDOP was 2.5 with minimum of 1.7 and maximum of 4.3. Fig. 3.1 shows the position difference computed by forward and backward solution from the local base station.

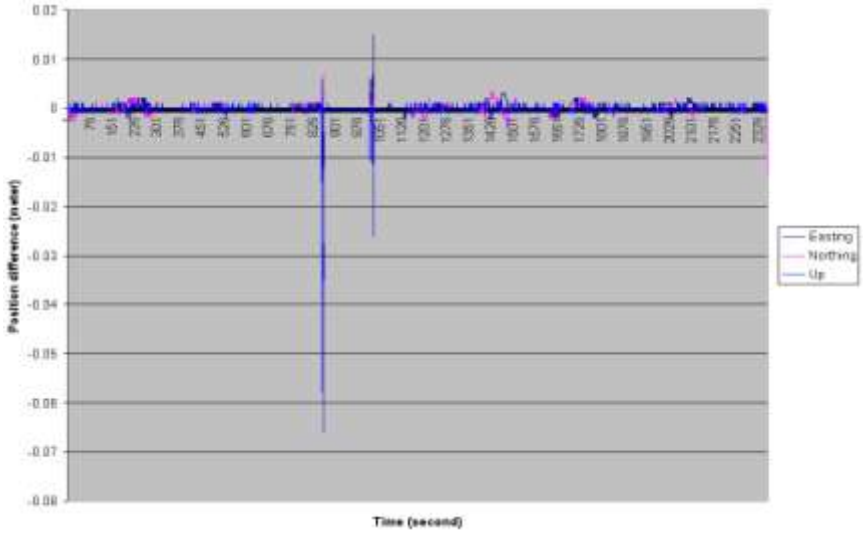

Fig. 3.1: Position difference at the local base station (meter)

To check the quality of the trajectory as a standard, position difference computed by two independent solutions (forward and backward solution) can be used when only one base station is available as this project was. Table 3.2 shows two solutions agreed with each other.

Table 3.2: Position difference computed by forward and backward solution (meter)

	Easting	Northing	Up
Average	0.00001	0.00000	0.00015
RMSE	0.00090	0.00078	0.00248

Fig. 3.2 and Table 3.3 shows a plot of position difference computed between the local base station and the reference station (NATA) without barometric data and statistics respectively.

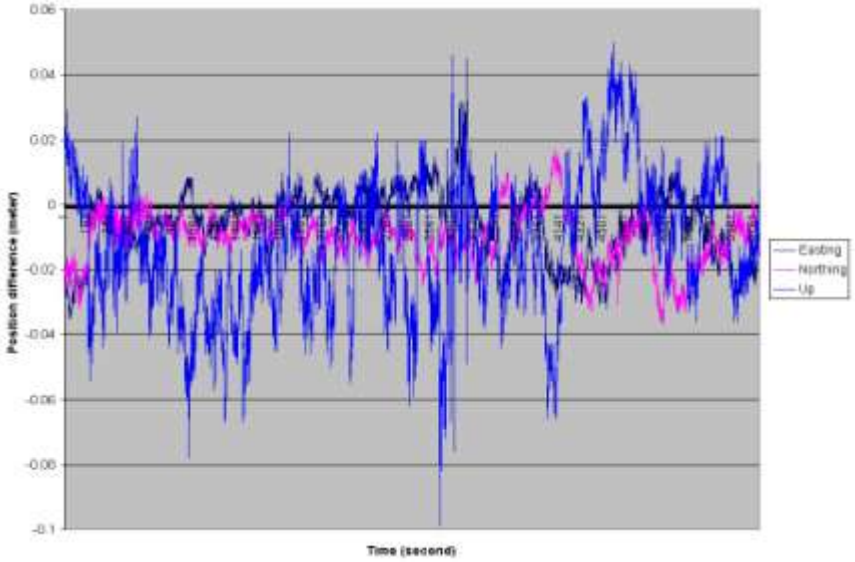

Fig. 3.2: Position difference computed without barometric data (meter)

Table 3.3: Position differences computed without barometric data

	Easting	Northing	Up
Average (m)	-0.0058	-0.0102	-0.0135
RMSE (m)	0.0106	0.0080	0.0210

Fig. 3.3 and Table 3.4 shows position difference computed between the local base station and NATA with barometric data. Trajectory computed from NATA with barometric data is closer to the standard than trajectory computed from the local base station.

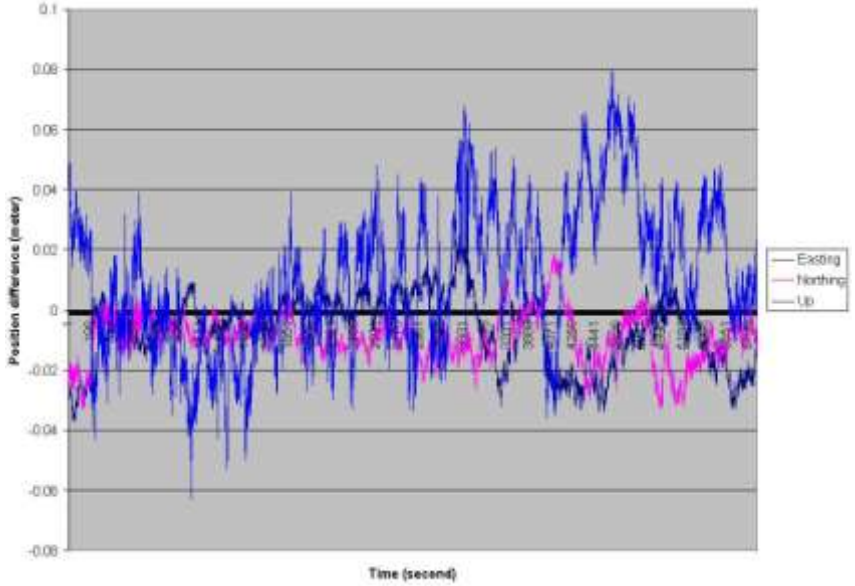

Fig. 3.3: Position difference computed with barometric data (meter)

Table 3.4: Position difference computed with barometric data

	Easting	Northing	Up
Average (m)	-0.0062	-0.0091	0.0105
RMSE (m)	0.0116	0.0080	0.0239

Fig. 3.4 and Table 3.5 shows position difference computed with and without barometric data from NATA to the project site.

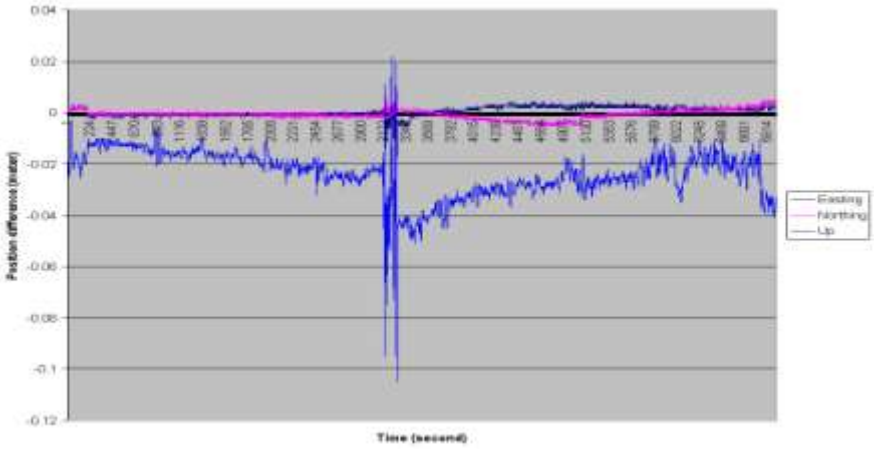

Fig. 3.4: Position difference computed with and without barometric data(meter)

Table 3.5: Position difference computed with and without barometric data

	Easting	Northing	Up
Average (m)	0.0006	-0.0006	-0.0237
RMSE (m)	0.0018	0.0018	0.0091

Raw barometric data was modified by addition and subtraction of 2.5 and 5.0 mbar to check how sensitive the trajectory to barometric data. Table 3.6 through Table 3.10 is statistics of position difference computed after modification. As in Fig. 3.5 and Table 3. 11 subtraction of 2.5 mbar from the original barometric data shows the closest to the standard trajectory.

Table 3.6: Addition of 5.0 mbar

	Easting	Northing	Up
Average (m)	-0.0071	-0.0087	0.0335
RMSE (m)	0.0127	0.0083	0.02704

Table 3.7: Addition of 2.5 mbar

	Easting	Northing	Up
Average (m)	-0.0066	-0.0089	0.0220
RMSE (m)	0.0121	0.00811	0.02537

Table 3.8: No modification

	Easting	Northing	Up
Average (m)	-0.0062	-0.0091	0.0105
RMSE (m)	0.0116	0.0080	0.0239

Table 3.9: Subtraction of 2.5 mbar

	Easting	Northing	Up
Average (m)	-0.0058	-0.0094	-0.0010
RMSE (m)	0.0110	0.0079	0.0228

Table 3.10: Subtraction of 5.0 mbar

	Easting	Northing	Up
Average (m)	-0.0054	-0.0096	-0.0126
RMSE (m)	0.0106	0.0079	0.0219

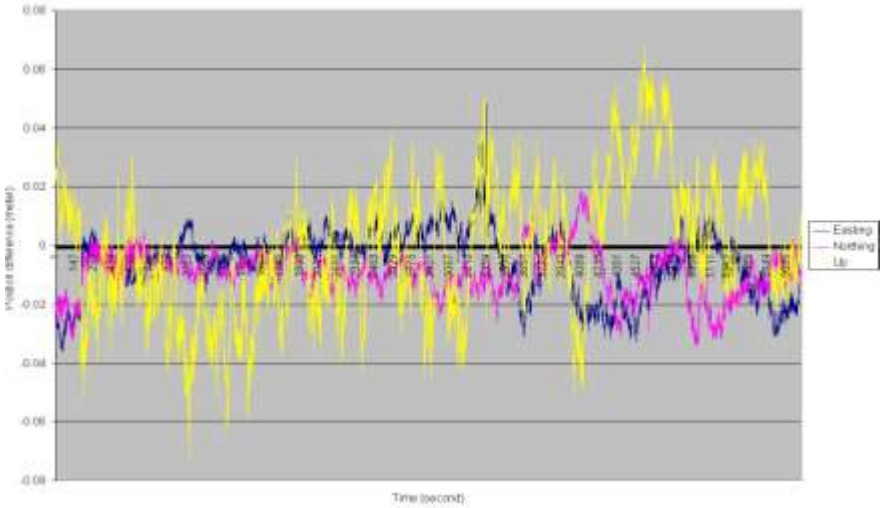

Fig.3.5: Position differences computed with modified barometric data (meter)

Table 3.11: Position differences computed with modified barometric data

	Easting	Northing	Up
Average (m)	-0.0066	-0.0094	-0.0010
RMSE (m)	-0.0110	0.0079	0.0227

IV. CONCLUSION

Although the statistical results of the position difference between the local base station and NATA with and without barometer data were less then desired or expected, it has been demonstrated that under proper conditions it might improve accuracy of aircraft positions over long base line.

The statistical results of Jacksonville project indicate 2.5 mbar subtracted from raw barometric data used for trajectory computed from NATA shows about fivemillimeter in easting, threemillimeter in northing and one centimeter in up improvements from the trajectory computed from local base station (Fig. 3.5 and Table 3.7). From natural of GPS characteristics, accuracy of height component is always worse than that of horizontal component. According to the results of this research, the height component is relatively improved much more then easting and northing component.

There were no significant difference of pressure between NATA and project sites. It might need to be a big front to see the effect of the tropospheric delay significantly. There are a lot of various other mapping functions such as Saastamoinen's, Ifadis's and Niell's available. Since each of the mapping functions is different from another it might be good to use other model and mapping functions other than just Marini's. This research shows that it is important to precisely measure precisely barometric pressure on the aircraft in motion.

With the present results of this research projects, following recommendations may be implemented to obtain better results.

1. Proper mission plan for better satellite geometry.
2. Significantly different surface conditions between base station and rover.
3. Different tropospheric models in KARS.
4. Precisely measurement of barometric pressure on the aircraft.

Although the cut-off angle was set as 15 degrees a couple of rising satellites right after above cut-off angle might cause some noise for a while when data were processed. Itis recommendedto plan properly before starting a project. Over pressure or under pressure might affect the accuracy of the aircraft positions. Because if the static source is located in an area producing higher than true (surrounding atmosphere) static pressure, the barometer will read lower pressure than it should. Conversely, a static source producing lower than true static pressure will cause higher barometric pressure than it should. This might be a case of this project.

V. Acknowledgements

The author would like to thank to Ramesh Shrestha, William Carter, and Michael Sartori for the laboratory facilities and advisement.

References

[1]. Collins, P.; Langley, R, B.; and LaMance, J. Limiting factors in tropospheric propagation delay error modeling for GPS airborne navigation, Proc. The institute of Navigation 52nd annual meeting, Cambridge, Massachusetts, 1996.

[2]. Collins, P.; and Langley, R.B. Estimating the residual tropospheric propagation delay for airborne differential GPS positioning,Proc. 10th International Technical Meeting of the Satellite Division of the Institute of Navigation, Kansas City, Missouri., 1997

[3]. Jensen, A.B.O., Real time modeling of the troposphere for network RTK,Geodetic Department, Kort & Matri kelstyrelsen Rentemestervej 8, DK-2400, kobenhavn NV, Denmark., 2000

[4]. Saha, K.; Raju, C.S.; and Parameswaran, K. A new hydrostatic mapping function for tropospheric delay estimation, Journal of Atmospheric and solar-Terrestrial Physics 72, 2010, 125-134.

[5]. Fernandes, M.J.; Pires, N.; Lázaro, C.; and Nunes, A.L. Tropospheric delays from GNSS for application in coastal altimetry. Advances in Space Research, 51,2013, 1352-1368.

[6]. Mendes, V.B.; and Langley, R.B. ,Optimization of troposheric delay mapping function performance for high-precision geodetic applications, Proc. DORIS Das,Toulouse, France., 1998.

[7]. Heinkelmann, R.; Bo¨hm, J.; Bolotin, S.; Engelhardt, G.; Haas, R.;Lanotte, R.; MacMillan, D.S.; Negusini, M.; Skurikhina, E.; Titov, O.; and Schuh, H. VLBI-derived troposphere parameters during CONT08. Journal of Geodesy, 85, 377–393.

[8]. Snajdrova, K.; Boehm, J.; Willis, P.; Haas, R.; and Schuh, H. Multi-technique comparison of tropospheric zenith delays derived during the CONT02 campaign. Journal of Geodesy, 79 (10–11), 2006, 613–623.

[9]. Teke, K.; Bo¨hm, J.; and Nilsson, T. Multi-technique comparison oftroposphere zenith delays and gradients during CONT08. Journal of Geodesy. 85, 2011, 395–413.

[10]. Willis, P.; Fagard, H.; and Ferrage, P. The International DORISService, first steps toward maturity. Advances in Space Research, 45 (12).,2010, 1408–1420.

[11]. Wang, C.S.; Liou, Y.A.; and Yeh, T.K. Impact of surface meteorological measurements on GPS height determination. Geophysical Research Letter 35, L23809.2008.

[12]. Leick, A. GPS satellite surveying, (New York: John Wiley &Sons Inc. 2015).

[13]. Morrison, R.A., Extended baseline on-the-fly ambiguity resolution using external double difference ionospheric information, Master's Thesis, University of Florida, Gainesville, FL, 2001.

[14]. Mader, G.L. Kinematic and rapid static (KARS) GPS positioning: Techniques and recent experiences. IAG Symposia No. 115, Boulder, CO, 1996, 170-174

Jinseok Hong" Estimation of Tropospheric Propagation Delay for Long Base Line in Gps Positioing" International Journal of Engineering Science Invention (IJESI), Vol. 08, No. 03, 2019, PP 01-10